

Supplementary Materials

Laser-Induced Graphene Arrays-Based Three-Phase Interface Enzyme Electrode for Reliable Bioassays

Man Zhang¹, Jun Zhang^{1,*}, Zhenyao Ding¹, Haili Wang¹, Lihui Huang¹ and Xinjian Feng^{1,2,*}

¹ College of Chemistry, Chemical Engineering and Materials Science, Soochow University, Suzhou 215000, China

² Innovation Center for Chemical Science, Soochow University, Suzhou 215000, China

* Correspondence: jzhang2017@suda.edu.cn (J.Z.); xjfeng@suda.edu.cn (X.F.)

Figure S1

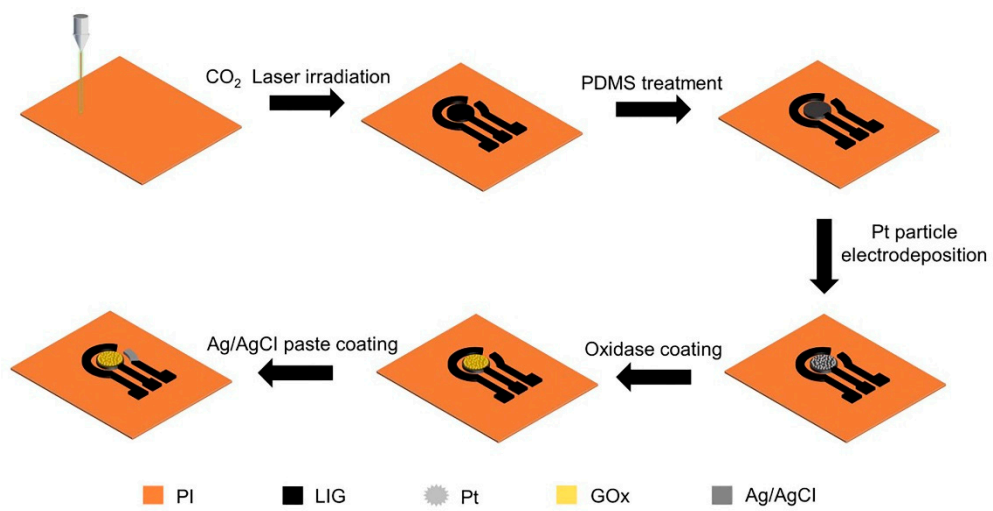


Figure S1. Fabrication process of the LIG-based three-phase biosensor.

Figure S2

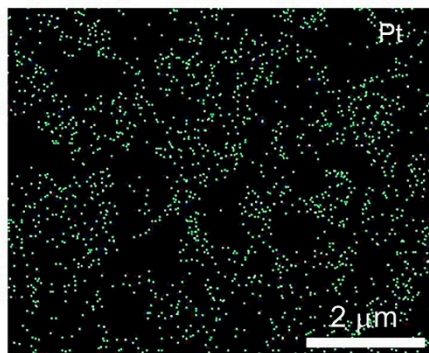


Figure S2. The elemental mapping (EDS) of hydrophobic LIG after Pt deposition.

Figure S3

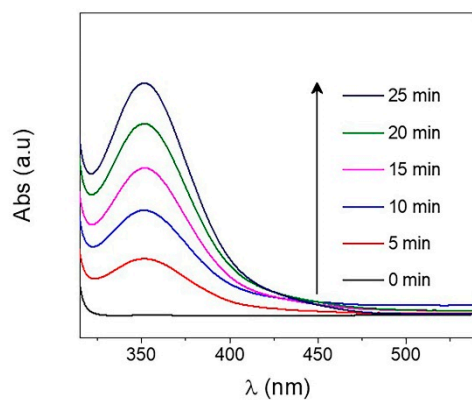


Figure S3. UV-vis absorption spectra of oxidase enzymatic product H₂O₂ in 20 mM glucose solution at different reaction times based on the diphasic electrode.

Figure S4

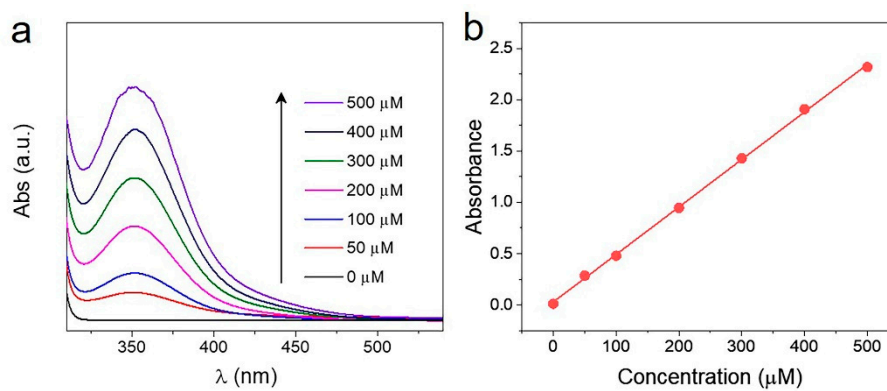


Figure S4. (a) UV-vis absorption spectra of different H_2O_2 concentrations. (b) The linear relationship between the absorbance and the H_2O_2 concentration.

Figure S5

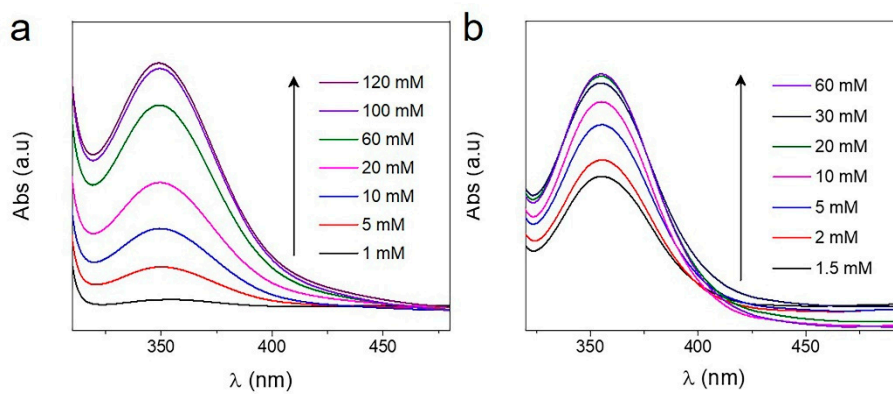


Figure S5. UV-vis absorption spectra of oxidase enzymatic product H_2O_2 at different glucose levels based on the three-phase (a) and diphasic (b) electrodes, respectively.

Figure S6

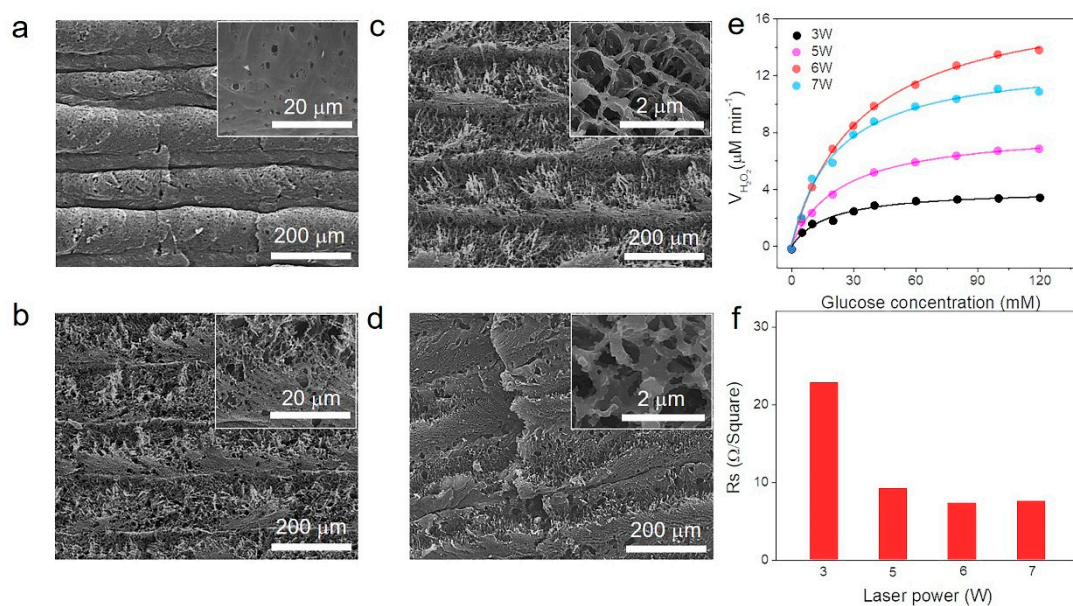


Figure S6. (a–d) The top microscopy images of the LIG substrates fabricated at 3, 5, 6, and 7 W powers. The insets show the magnified image of LIGs. (e) The functional relation of H_2O_2 production rate with glucose concentration based on the LIG-based three-phase systems at different powers. (f) The dependence of the sheet resistance of LIG on laser power.

Figure S7

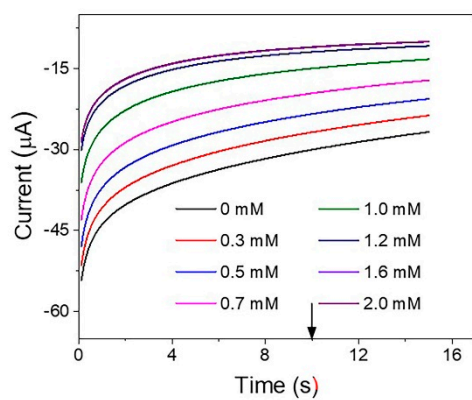


Figure S7. Amperometric response of the LIG-based diphasic biosensor in glucose solution with concentrations from 0 to 2 mM.

Figure S8

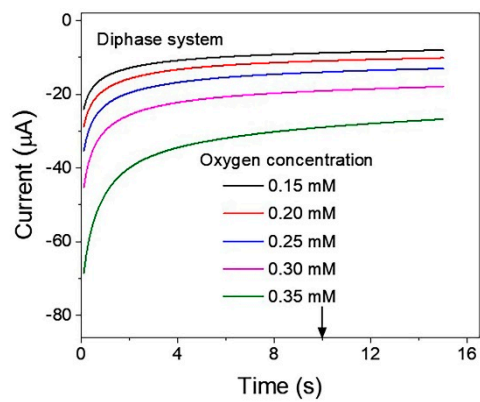


Figure S8. Amperometric responses of LIG-based conventional diphase biosensors in blank PBS solution with different oxygen contents.

Figure S9

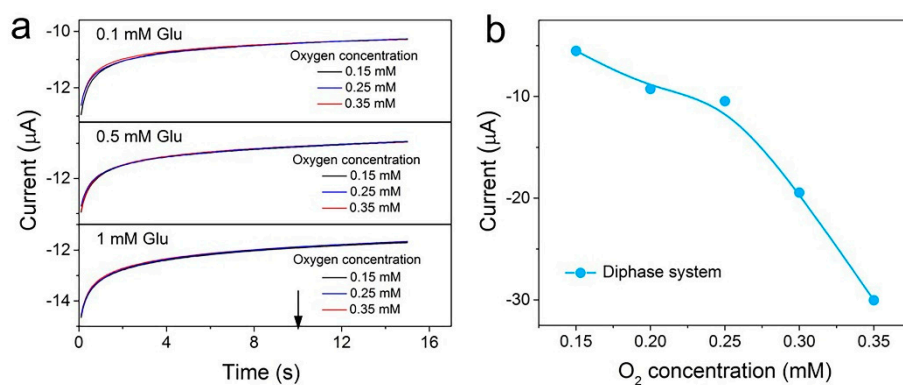


Figure S9. (a) Amperometric i - t curves of the LIG-based three-phase biosensor in 0.1, 0.5, and 1 mM glucose solution with various oxygen contents. (b) Amperometric responses of LIG-based diphase biosensors in 1 mM glucose solution with different oxygen levels.

Figure S10

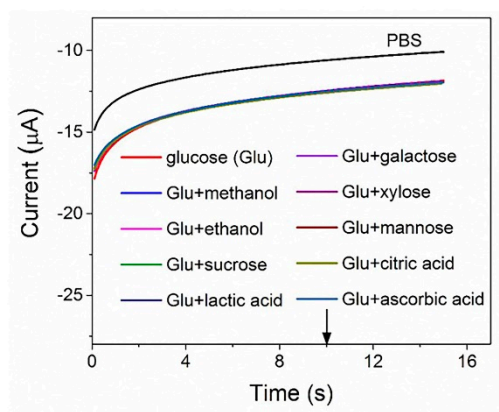


Figure S10. Amperometric $i-t$ response of the LIG-based three-phase biosensor at 0 V in PBS on addition of 1.0 mM glucose followed by 0.1 mM methanol, ethanol, sucrose, lactic acid, galactose, xylose, mannose, citric acid and ascorbic acid.

Figure S11

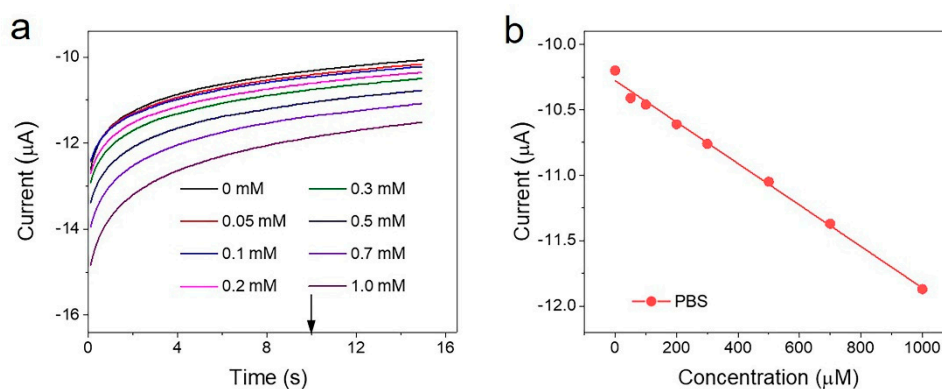


Figure S11. (a) Amperometric $i-t$ curves responses of the LIG-based three-phase biosensor in glucose solution with concentrations from 0 to 1 mM, (b) Corresponding calibration plot derived from (a) at 10 s.

Figure S12

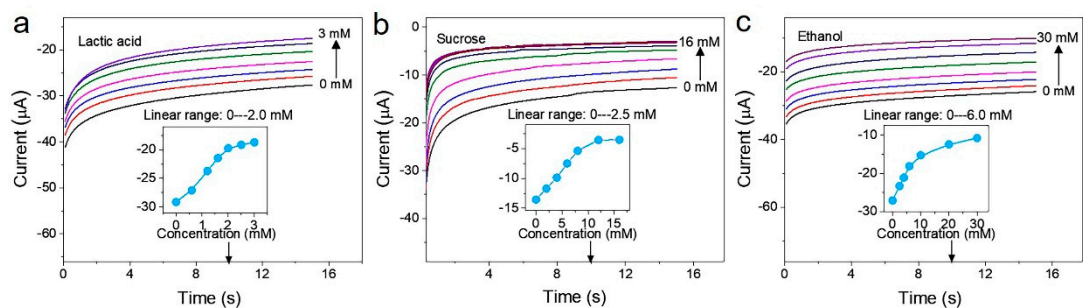


Figure S12. (a–c) Amperometric responses of the LIG-based diphasic biosensor in lactic acid, sucrose, and ethanol solutions, respectively. Insets are their corresponding calibration plots derived at 10 s.